



ORIGINAL PAPER

N-heterocyclic carbene-based polymer coating of gold nanoparticles and luminescent quantum dots

Neda Arabzadeh Nosratabad¹ · Zhicheng Jin¹ · Liang Du¹ · Hedi MattoSSI¹

Received: 23 November 2022 / Accepted: 22 March 2023
© The Author(s), under exclusive licence to The Materials Research Society 2023

Abstract

We test the capacity of two N-heterocyclic carbene (NHC)-based metal-coordinating compounds that present polyethylene glycol solubilizing blocks, a polymer and monomer, as ligands for the surface passivation of colloidal gold nanoparticles, luminescent quantum dots, and iron oxide nanoparticles (IONPs) alike in water. The long-term colloidal stability of the NHC-stabilized nanocolloids has been tested following phase transfer to aqueous media, which presents a highly challenging environment for such groups, due to the moisture-sensitive nature of NHC molecules. We find that nanocrystals coated with these NHC-containing ligands exhibit long-term colloidal stability in buffer media with no sign of degradation or aggregation build-up, while preserving their photo-physical properties, for extended periods of time.

Introduction

Inorganic nanocrystals have attracted much attention over the past 30 years, due to their potential use in various applications, such as optical and electronic devices, as well as in biology and biomedicine [1–4]. The photo-physical properties of these materials can be modified by tuning the dimensions, core composition, stoichiometry, and morphology of the colloids. For instance, CdSe–ZnS core shell QDs exhibit broad absorption along with narrow tunable emission throughout the visible spectrum. Their high quantum yield combined with resistance to photo- and chemical degradation have made them attractive for use as fluorescent probes in biomedical applications and for developing optoelectronic devices [5, 6]. Similarly, nanocrystals made of noble metals (e.g., AuNPs) possess unique optoelectrical properties due to their well-known localized surface plasmon resonance (LSPR) [7]. However, as-grown most inorganic nanocolloids are not readily transferrable between solvents with different polarities. One notable drawback is the very limited compatibility of as-grown nanocolloids with biological systems. A common strategy to overcome this issue has been the use of amphiphilic ligands to promote the dispersion of various inorganic nanocrystals in polar solvents and buffer

media, through cap exchange approaches. In recent years, N-heterocyclic carbenes (NHCs) have emerged as versatile metal-coordinating groups, due to their σ -donating nature as soft Lewis bases, which can coordinate with transition metal cores; these tend to possess soft Lewis acid character [8–10]. They have been actively employed for the surface passivation of variety of nanocrystal surfaces [11–15]. In this study, a new set of NHC-modified molecules have been prepared and used as surface-stabilizing ligands of AuNPs, IONPs, and luminescent QDs. We find that cap exchange using an NHC-polymer (multi-coordinating ligand) yields nanocrystals that exhibit long-term colloidal stability over a broad range of conditions.

Materials and methods

Reagents

Imidazole (99%) was purchased from Acros Organics (Morris Plains, NJ). All other chemicals and solvents were purchased from Sigma-Aldrich (St Louis, MO). Deuterated solvents used for NMR experiments were purchased from Cambridge Isotope Laboratories (Andover, MA). The chemicals and solvents were used as received unless otherwise specified. Column purification chromatography was performed using silica gel (60 Å, 230–400 mesh, purchased from Bodman Industries, Aston, PA).

✉ Hedi MattoSSI
mattoSSI@chem.fsu.edu

¹ Department of Chemistry and Biochemistry, Florida State University, 95 Chieftan Way, Tallahassee, FL 32306, USA

Synthesis of NHC-modified ligands

We limit our description to the preparation of the multi-NHC-polymer (compound 2). Synthesis of this compound relied on the ring opening nucleophilic addition reaction starting with poly(isobutylene-*alt*-maleic anhydride), PIMA, following the protocol described by our group [16]. It involved two steps: (1) Ring opening reaction between PIMA and a stoichiometric mixture of aminopropyl ethyl imidazolium (APEIm-iium) and NH₂-PEG-OMe nucleophiles to yield APEIm-iium-PIMA-PEG polymer. (2) Transformation of APEIm-iium-PIMA-PEG to NHC-PIMA-PEG during the ligand exchange for AuNPs, where carbene generation was carried out in the presence of the NPs (i.e., *in situ*) under strong basic conditions. A monomeric PEG-imidazolium salt (PEG-EIm-iium) was also prepared [11].

Cap exchange of OLA-AuNPs with NHC-PIMA-PEG polymer

OLA-AuNP dispersions (75 μ L, 0.67 μ M) were precipitated using excess EtOH and redispersed in THF (400 μ L). This solution was mixed with 400 μ L of THF containing 19 mg of APEIm-iium-PIMA-PEG using a scintillation vial. The vial was sealed and then subjected to 2–3 rounds of purging with N₂ followed by a mild vacuum, in order to switch the atmosphere to N₂. Then, 3 mg of KOtBu dissolved in dry THF (600 μ L) was added dropwise to promote *in situ* carbene generation. The mixture was then stirred at 40 °C overnight and then the NHC-PIMA-PEG-coated AuNPs were precipitated by adding excess hexane. One round of centrifugation at 3500 RPM for 2 min was applied yielding a dark precipitate. The clear supernatant was discarded, and the pellet was redispersed in ~500 μ L of THF, followed by precipitation using excess hexane. This procedure was repeated one more time. The residual precipitate was gently dried under nitrogen flow and then dispersed in DI water. The aqueous dispersion was filtered using 0.45- μ m disposable syringe filter. Then, two rounds of concentration/dilution using a membrane centrifugal filtration device (Amicon Ultra, 100 kDa) were applied to purify the NHC-PIMA-PEG-AuNP dispersions from excess ligands. The oleylamine-coated AuNPs were grown using high-temperature reaction as previously reported [17]. A similar approach was used to prepare NHC-PEG-stabilized AuNPs, but starting with monomeric PEG-EIm-iium ligand (compound 1).

Cap exchange of QDs with NHC-PIMA-PEG polymer

Ex *situ* conditions were used for ligand exchange of as-grown QDs with NHC-polymer, where carbene groups

were first generated in the absence of QDs. Hydrophobic stock dispersion of red-emitting TOP/TOPO-QDs (100 μ L, 9.8 μ M) were first purified from excess native ligands using ethanol and redispersed in 50 μ L of CHCl₃. Separately, 15 mg of NHC-PIMA-PEG was dissolved in CHCl₃ (100 μ L) and added to the QD dispersion. This mixture was sonicated for 5 min, and excess hexane was added. One round of centrifugation at 5000 RPM for 2 min was applied to precipitate the newly formed NHC-PIMA-PEG-QDs. After discarding the clear supernatant, the pellet was redispersed in ~150 μ L of CHCl₃. This procedure was applied twice. The final precipitate was dried under mild vacuum and dispersed in DI water. The hydrophilic NHC-PIMA-PEG-coated QDs were purified from excess free ligands by applying 2–3 rounds of concentration/dilution using a membrane centrifugal filtration device with DI water. The Core–shell CdSe–ZnS quantum dots were synthesized following reported strategies using hot injection techniques [18, 19].

Cap exchange of IONPs with NHC-PIMA-PEG polymer

150 μ L of oleic acid-capped iron oxide nanoparticles were precipitated using excess ethanol. The precipitate containing the nanoparticles was dispersed in 400 μ L of THF and then mixed with 500 μ L of THF containing 43 mg of APEIm-iium-PIMA-PEG. The vial was sealed, and the atmosphere was switched to nitrogen. Then, 9 mg of KOtBu dissolved in 700 μ L of dried THF was added dropwise to promote *in situ* carbene generation. The content was stirred at 40 °C overnight. The sample was precipitated using excess hexane. Following sonication for ~1 min, the dispersion was centrifuged at 3700 RPM for ~5 min, yielding a pellet. The procedure was repeated one more time. The residual precipitate was dried under N₂ flow and dispersed in ~3–5 mL of DI water. The obtained clear aqueous dispersion of IONPs was first passed through a 0.45- μ m syringe filter. Then, excess free ligands were removed by applying 3–4 rounds of concentration/dilution (DI water), as done above. The iron oxide NPs used were prepared following the steps detailed in reference [20].

Results and discussion

Ligand design

A commercially available imidazole derivative has been selected as the NHC precursor because it allows easy functionalization of the two nitrogen atoms within the imidazole ring. Also, the substituents bound to the nitrogen atoms next to carbene center help the kinetic stabilization of these species by sterically hindering the dimerization to the corresponding olefin [21]. Due to the inherent electron-donating

property of NHC, such molecules are considered soft Lewis base and thus exhibit strong affinity (via soft-to-soft) to transition metal surfaces (which exhibit a soft Lewis acidic character). Hence, we designed two sets of NHC-based ligands: a monodentate NHC-PEG and a multi dentate NHC-PIMA-PEG as shown in Fig. 1.

The monodentate ligand (compound 1) was synthesized by alkylation of PEG-appended imidazole using ethyl bromide. Then, *in situ* conversion of this product (compound 1) to NHC-PEG was carried out in the presence of KOTBu during the ligand exchange process. The polymer ligand was prepared via the one-step nucleophilic addition reaction between PIMA and several primary amine-containing moieties [16, 22]. Synthesis starts by reacting PIMA with pre-synthesized H₂N-PEG and APEIm-ium to yield APEIm-ium-PIMA-PEG (compound 2, serving as an intermediate). Following deprotonation of the C-2 proton using KOTBu, the resulting modular ligand presents multiple NHC-anchoring groups and hydrophilic PEG motifs.

Characterization of the NHC-coated nanocrystals

Surface modification of oleylamine-AuNPs, oleic acid-IONPs, and TOP/TOPO-capped CdSe-ZnS QDs with the NHC-based ligands was carried out using one-phase ligand exchange in THF or CHCl₃. Ligand substitution of OLA-AuNPs and OA-IONPs was carried out under *in situ* conditions, where carbene transformation in the presence of KOTBu was combined with the ligand exchange reaction. In comparison, ligand substitution of TOP/TOPO-QDs was

carried out under *ex situ* conditions using preformed NHC-PIMA-PEG; here, the NHC groups were first generated (using KOTBu) prior to mixing with the QDs.

OA-IONPs were first mixed with excess molar concentration of APEIm-ium-PIMA-PEG with respect to IONPs under inert atmosphere (in THF). Then, a solution of KOTBu dissolved in THF was added dropwise through a septum to promote deprotonation of the APEIm-ium-PIMA-PEG salts and a mild overnight heating was used. Similar ligand exchange protocols were applied for the NHC-PEG-AuNPs starting with OLA-AuNPs.

The newly coated AuNPs were characterized using NMR spectroscopy, optical spectroscopy, and dynamic light scattering (DLS) measurements. Figure 2A shows a few representative ¹H NMR spectra collected from solutions of the precursor, APEIm-ium-PIMA-PEG, side by side with a dispersion of the corresponding NHC-PIMA-PEG-stabilized AuNPs after phase transfer to D₂O (bottom). The spectrum acquired from solution of APEIm-ium-PIMA-PEG shows two distinct peaks: one at 7.59 ppm attributed to the merged ring protons (i and j), while the signature at 8.87 ppm is assigned to the C-2 proton (h). The data collected from the NHC-PIMA-PEG-AuNP dispersions show that the acidic proton peak (h) is absent from the NHC-polymer-ligated AuNP dispersions. This provides strong evidence for the carbene generation and coordination of NHC-ligands on the AuNP surfaces (see Fig. 2A, bottom spectrum). Similarly, the ¹H NMR spectrum acquired from the NHC-polymer-stabilized QDs shows characteristic peaks ascribed to the PEG blocks (at ~ 3.3 ppm ascribed to the OMe protons and at 3.6 ppm

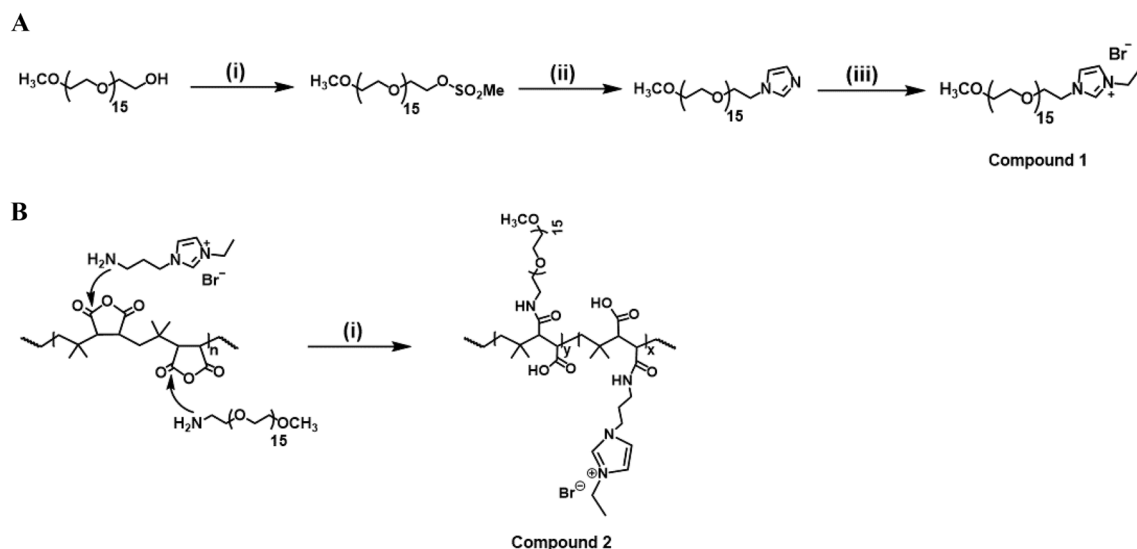


Fig. 1 Synthetic steps employed for preparing NHC-based ligands. **A** steps involved in the synthesis of the PEG-EIm-ium monomer, (i) MsCl, Et₃N, THF; (ii) imidazole, NaOH, THF, reflux (4 h); and (iii) ethyl bromide, THF, reflux (4 h). This compound was further

used to prepare the NHC-PEG ligand. **B** Synthesis of APEIm-ium-PIMA-PEG starting with PIMA, H₂N-PEG-OCH₃, and APEIm-ium, (i) DMSO, 50 °C. We note that the NHC-PEG and NHC-PIMA-PEG were generated *in situ* in the presence of the nanocrystals

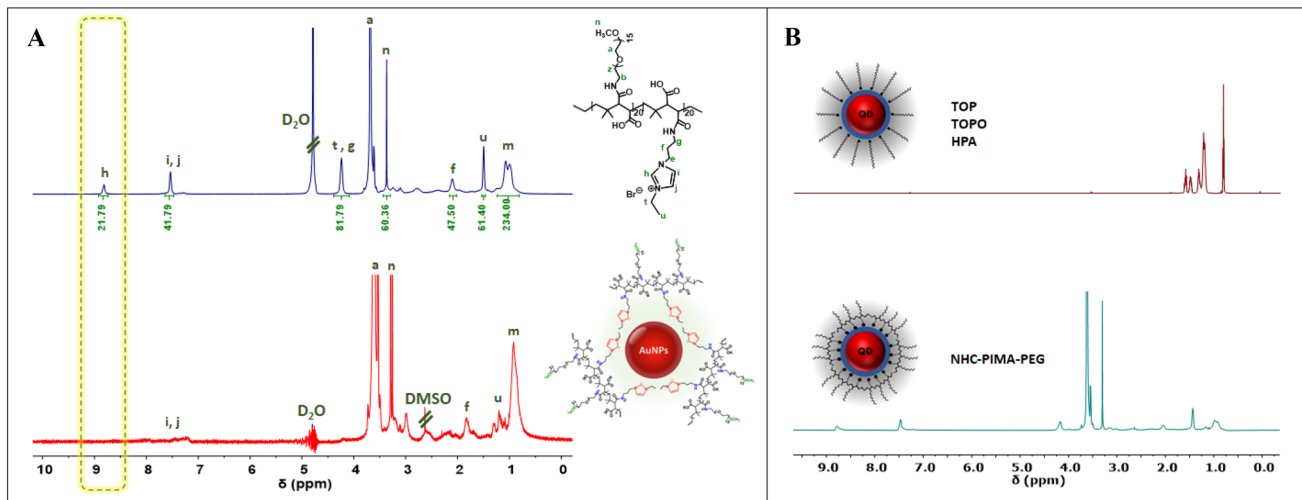


Fig. 2 Stacked ^1H NMR spectra measured for **A** APEIm-ium-PIMA-PEG prior to carbene generation and NHC-PIMA-PEG-AuNPs; **B** QD dispersions before and after ligand exchange, collected in CDCl_3

emanating from the $\text{CH}_2\text{-CH}_2\text{-O}$ protons), the PIMA chain dimethyl protons (at $\sim 0.9\text{-}1$ ppm), and two merged NHC ring protons (at ~ 7.5 ppm), see Fig. 2B (bottom spectrum). In comparison, the spectrum of the hydrophobic QDs shows only signatures at $\sim 0.5\text{-}1.75$ ppm ascribed to the native ligands, namely a mixture of TOP, TOPO, HDA, and HPA protons [23]. We note that the NMR spectrum acquired from NHC-polymer-ligated QDs in D_2O shows a weak signature at 9.24 ppm ascribed to the acidic proton (C-2) in the imidazole ring, which implies that a small fraction of NHC molecules have reversed back to imidazolium. Nonetheless, the integrity of the NHC-polymer-QDs in water was preserved. This indicates that the remaining NHC groups along the chain ($\sim 14\text{-}15$ per ligand) are still able to promote strong and stable binding onto the QD surfaces.

The absorption and/or emission spectra collected from dispersions of AuNPs and QDs before and after ligand substitution with NHC-PEG or NHC-PIMA-PEG ligands are shown in Fig. 3A-C. The absorption and emission spectra acquired for the hydrophilic nanocrystals exhibit essentially identical features to those collected from the native hydrophobic samples, which proves that the optical integrity of the nanocrystals has been preserved after stabilization with NHC-ligands (see Fig. 3A-C). Figure 3E and F shows histograms of the intensity versus hydrodynamic radius (R_{H}) generated from the Laplace transform of the autocorrelation function of the scattered laser intensity measured for NHC-PIMA-PEG-capped AuNPs/IONPs. Single peaks were measured for both dispersions, indicating that the resulting dispersions are homogeneous and aggregate free, similar to the histogram measured for the starting hydrophobic dispersion. In comparison, the DLS data acquired from

or D_2O , respectively. Water suppression was applied to the spectra collected from the aqueous samples

NHC-PEG-AuNPs shows that two populations of scattering objects are present: a narrow one corresponding to smaller colloids (single nanoparticles) and another generated by a small fraction of stable aggregates formed in the dispersion (see Fig. 3D). All in all, these results combined indicate that surface stabilization using NHC-based ligands maintains the integrity and homogeneity of all three types of nanocolloids.

Colloidal stability tests

Colloidal stability tests were applied to aqueous nanocrystals capped with NHC-PIMA-PEG and prepared under several biologically relevant conditions, including pH changes, high ionic strength solution, and in the presence of dithiothreitol, DTT (a commonly known reducing agent). Figure 4A-C shows white light images of dispersions of NHC-PIMA-PEG-coated AuNPs, IONPs, along with fluorescence images collected from red-emitting QD dispersions in buffers over pH 3–12, in 1-M NaCl, 0.1-M DTT, and DI water. These images indicate that NHC-polymer-coated AuNPs remained homogeneous and free of aggregate for a period that exceeds one year of storage, while dispersions of QDs ligated with NHC-PIMA-PEG remained homogeneous and fluorescent under all tested conditions, except the one at pH 3, which exhibits a reduced fluorescence albeit without loss of colloidal stability (see Fig. 4C). The weaker fluorescence image measured at pH 3 can be attributed to partial protonation of the NHC groups in acidic conditions, resulting in partial back conversion to imidazolium molecules. As imidazolium groups exhibit weak to no coordination onto the QDs, coating of the QDs with these ligands results in more exposed surfaces and loss in PL. The white

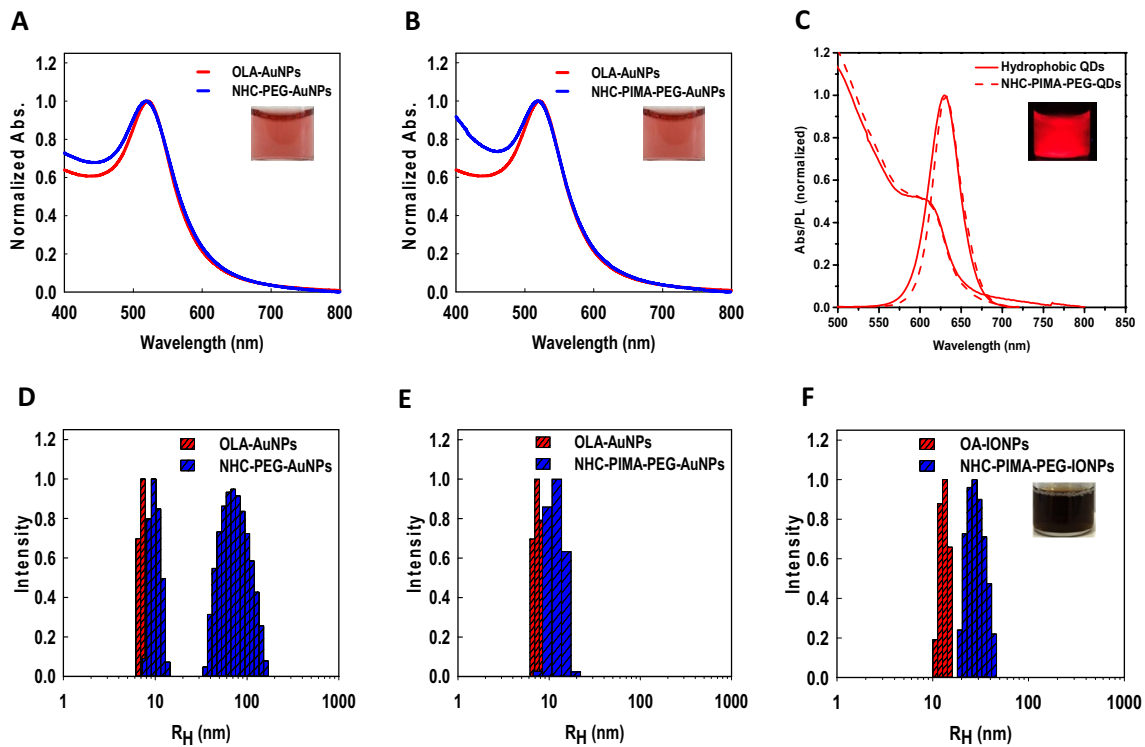


Fig. 3 **A–C** Optical characterization of AuNPs and QDs before and after ligand exchange with NHC-PEG or NHC-PIMA-PEG and transfer to aqueous media. Insets in panels **A** and **B** show white light images of hydrophilic AuNPs, while inset in panel **C** shows a fluorescence image of QD dispersion acquired under UV illumination

using a hand-held UV lamp. **D–F** Histograms showing the distribution of intensity versus hydrodynamic radius measured for AuNPs and IONPs, before and after cap exchange with NHC-PEG and NHC-PIMA-PEG. The inset in panel **F** shows a white light image of a dispersion of IONPs coated with NHC-PIMA-PEG

light images acquired from dispersions of the NHC-polymer-IONPs shown in Fig. 4B indicate that even though the dispersions stayed stable over the pH range 3–9, and in 1-M NaCl for 60 days, there was aggregation build-up after 80 days of storage. Time progression of the intensity vs size histograms obtained from dispersions of gold nanoparticles capped with NHC-PIMA-PEG shows that the hydrodynamic radii measured for all tested conditions essentially stayed constant throughout the test period of 1 year, see Fig. 4D. In comparison, the histogram acquired from the monomer-stabilized AuNPs (NHC-PEG-AuNP dispersions) shows a bimodal distribution throughout the test period, which is attributed to the presence of a small fraction of stable aggregates in the system [11].

We would like to emphasize the ability of DLS as an analytical technique to identify the presence of a small fraction of aggregates in the NHC-PEG-capped AuNP dispersions, even though the UV–Vis absorption profile of this sample is identical to that collected from OLA-AuNPs in organic media (see Fig. 3A). This indicates that those aggregates are small and colloidally stable. The gel electrophoresis image in Fig. 4F shows single and narrow gel mobility bands under all conditions tested, which provides further proof that the

dispersions of the NHC-polymer-stabilized QDs are homogeneous and stable.

Conclusion

We have designed and synthesized two sets of NHC-based metal-coordinating ligands, consisting of one monomer and one polymer, and tested their ability to promote colloidal stabilization of different types of inorganic nanocrystals in aqueous media. The nanocrystals have various transition metal cores, such as Au nanoparticles, luminescent CdSe–ZnS QDs, and iron oxide nanoparticles. We applied a few analytical techniques including ^1H NMR spectroscopy, fluorescence spectroscopy, and dynamic light scattering to characterize the ligands and further probe the nature of the binding interactions. Our results show that the NHC-polymer coating is particularly effective in promoting longer-term colloidal stabilization for all three types of nanocolloids in buffer media under a wide range of conditions. We should note that the long-term stability data exhibited by the prepared nanocrystals in aqueous media (a very destabilizing environment for free NHC groups) reflects the strong

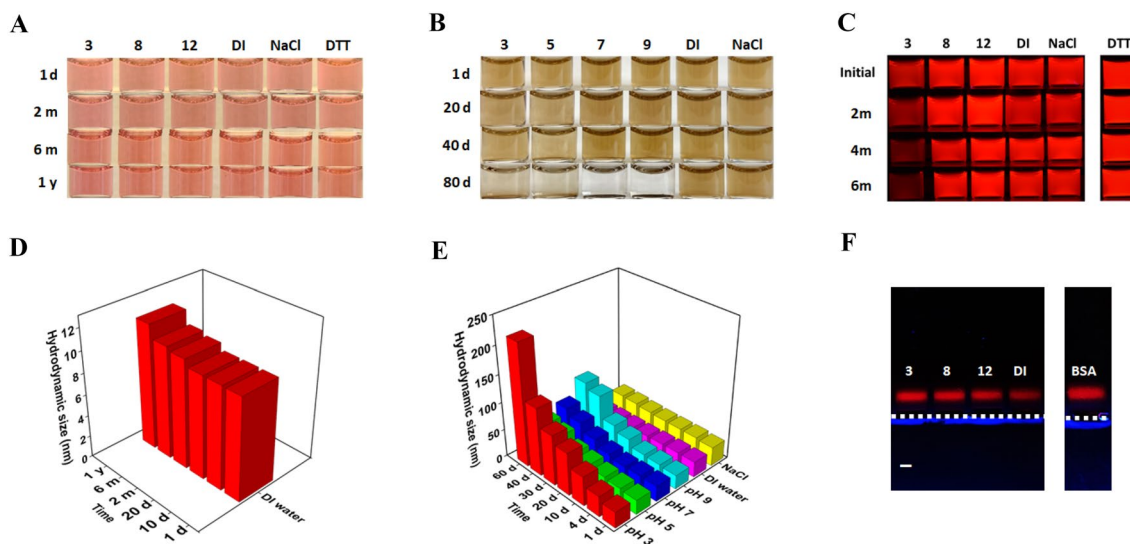


Fig. 4 **A–C** Colloidal stability tests applied to AuNPs, IONPs, and QDs ligand exchanged with NHC-PIMA-PEG and dispersed under varying conditions. Shown are dispersions in four different pH buffers, DI water, 1-M NaCl solution, and 0.1-M DTT solution. The fluorescence images of the QD samples were acquired under UV illumination using a hand-held UV lamp with excitation at 365 nm. **D** Hydrodynamic radius measured from NHC-PIMA-PEG-AuNP dispersions in DI water at different storage times. **E** Time progression of the apparent hydrodynamic radius measured from NHC-PIMA-PEG-IONP dispersions in different pH buffers, in DI water and in 1-M

NaCl solution. **F** Agarose gel electrophoresis images of NHC-PIMA-PEG-QD dispersions. Gel electrophoresis measurements were run on a 0.6% agarose gel using tris-borate EDTA buffer at different pH side by side with DI water. A control well on the right was loaded with a dispersion of QDs mixed with BSA and pre-incubated for 1 h. The dashed line designates the location of the loading wells. Images were collected under fluorescence mode as shown in panel C. The narrow bands and identical mobility shift observed for all wells imply that NHC-PIMA-PEG-QD dispersions in all pH media are homogeneous and aggregate free

and stable coordination interactions exhibited by the NHC groups toward all three sets of transition metal cores. The stable Au-to-NHC bond formation is a feature that can be attributed to the soft Lewis base character of NHC groups, which matches favorably with the soft Lewis acidic nature of the nanocolloid surfaces.

Acknowledgments The authors thank FSU and the National Science Foundation (NSF-CHE #2005079) and Kasei-Asahi for financial support.

Declarations

Conflict of interest The authors declare no competing financial interest.

References

1. P.K. Jain, X. Huang, I.H. El-Sayed, M.A. El-Sayed, *Plasmonics* (2007). <https://doi.org/10.1007/s11468-007-9031-1>
2. M.-C. Daniel, D. Astruc, *Chem. Rev.* (2004). <https://doi.org/10.1021/cr030698>
3. I.L. Medintz, H.T. Uyeda, E.R. Goldman, H. Mattoussi, *Nat. Mater.* (2005). <https://doi.org/10.1038/nmat1390>
4. Y. Shirasaki, G.J. Supran, M.G. Bawendi, V. Bulović, *Nat. Photon.* (2013). <https://doi.org/10.1038/nphoton.2012.328>
5. W. Wang, H. Mattoussi, *Acc. Chem. Res.* (2020). <https://doi.org/10.1021/acs.accounts.9b00641>
6. C.-H.M. Chuang, P.R. Brown, V. Bulović, M.G. Bawendi, *Nat. Mater.* (2014). <https://doi.org/10.1038/nmat3984>
7. R. Sardar, A.M. Funston, P. Mulvaney, R.W. Murray, *Langmuir* (2009). <https://doi.org/10.1021/la9019475>
8. P. Pyykkö, N. Runeberg, *Chem. Asian J.* (2006). <https://doi.org/10.1002/asia.200600181>
9. M. Rodríguez-Castillo, G. Lugo-Preciado, D. Laurencin, F. Tielens, S. Clément, Y. Guari, J.M. López-De-Luzuriaga, M. Monge, F. Remacle, S. Richeter, *Chem. Eur. J.* (2016). <https://doi.org/10.1002/chem.201601253>
10. A.V. Zhukhovitskiy, M.G. Mavros, T. Van Voorhis, J.A. Johnson, *J. Am. Chem. Soc.* (2013). <https://doi.org/10.1021/ja401965d>
11. N.A. Nosratabad, Z. Jin, L. Du, M. Thakur, H. Mattoussi, *Chem. Mater.* (2021). <https://doi.org/10.1021/acs.chemmater.0c03918>
12. L. Du, N.A. Nosratabad, Z. Jin, C. Zhang, S. Wang, B. Chen, H. Mattoussi, *J. Am. Chem. Soc.* (2021). <https://doi.org/10.1021/jacs.0c10592>
13. N. Arabzadeh Nosratabad, Z. Jin, L. Du, H. Mattoussi, *SPIE BiOS* (2022). <https://doi.org/10.1117/12.2610485>
14. J.-F. Soule, H. Miyamura, S. Kobayashi, *J. Am. Chem. Soc.* (2013). <https://doi.org/10.1021/ja404006w>
15. A. Rühling, K. Schaepe, L. Rakers, B. Vonhören, P. Tegeder, B.J. Ravoo, F. Glorius, *Angew. Chem. Int. Ed.* (2016). <https://doi.org/10.1002/anie.201508933>
16. W. Wang, A. Kapur, X. Ji, M. Safi, G. Palui, V. Palomo, P.E. Dawson, H. Mattoussi, *J. Am. Chem. Soc.* (2015). <https://doi.org/10.1021/jacs.5b00671>
17. S. Liu, G. Chen, P.N. Prasad, M.T. Swihart, *Chem. Mater.* (2011). <https://doi.org/10.1021/cm201343k>
18. C. Murray, D.J. Norris, M.G. Bawendi, *J. Am. Chem. Soc.* (1993). <https://doi.org/10.1021/ja00072a025>

19. Z.A. Peng, X. Peng, *J. Am. Chem. Soc.* (2001). <https://doi.org/10.1021/ja003633m>
20. J. Park, K. An, J.-G.P.Y. Hwang, H.-J. Noh, J.-Y. Kim, J.-H. Park, N.-M. Hwang, T. Hyeon, *Nat. Mater.* (2004). <https://doi.org/10.1038/nmat1251>
21. M.N. Hopkinson, C. Richter, M. Schedler, F. Glorius, *Nature* (2014). <https://doi.org/10.1038/nature13384>
22. L. Du, S. Helsper, N.A. Nosratabad, W. Wang, D.A. Fadool, C. Amiens, S. Grant, H. Mattossi, *Bioconjug. Chem.* (2022). <https://doi.org/10.1021/acs.bioconjchem.2c00116>
23. B. Zeng, G. Palui, C. Zhang, N. Zhan, W. Wang, X. Ji, B. Chen, H. Mattossi, *Chem. Mater.* (2018). <https://doi.org/10.1021/acs.chemmater.7b04204>

Publisher's Note Springer Nature remains neutral with regard to jurisdictional claims in published maps and institutional affiliations.

Springer Nature or its licensor (e.g. a society or other partner) holds exclusive rights to this article under a publishing agreement with the author(s) or other rightsholder(s); author self-archiving of the accepted manuscript version of this article is solely governed by the terms of such publishing agreement and applicable law.